Mode selectivity and stability of continuously pumped atom lasers

S. A. Haine* and J. J. Hope
Australian Centre for Quantum Atom Optics, Department of Physics, Australian National University, ACT 0200, Australia
(Received 6 April 2003; published 25 August 2003)

A semiclassical, multimode model of a continuously pumped atom laser is presented. For a spatially independent coupling process it is found that the system is unstable below a critical scattering length. As large atomic interactions will increase the phase diffusion of the lasing mode, it is desirable to obtain a stable atom laser with low nonlinearity. It is shown that spatially dependent pumping stabilizes the atom laser to a finite number of modes, and can induce single-mode operation.

DOI: 10.1103/PhysRevA.68.023607 PACS number(s): 03.75.Pp, 03.65.Sq, 05.45.−a

I. INTRODUCTION

The recent development of the atom laser [1–6] has opened up the possibility of a revolution in atom optics just as the optical laser revolutionized photon optics. The useful characteristics of optical lasers such as mode selectivity, temporal coherence, and high spectral density occur for the atom laser. The last two properties in particular will be vastly improved by the realization of a truly continuous atom laser [7]. For an optical laser to have minimum linewidth and hence maximum spectral flux, it must be continuously pumped and come to steady state in a single-mode operation [8]. In this paper we show that a continuously pumped atom laser will only achieve a single-mode steady state under certain conditions.

Atom lasers have been demonstrated experimentally by outcoupling atoms from Bose-Einstein condensates (BEC) in magnetic traps. This is done by changing the internal state of the atom to one that is either untrapped or antitrapped [2–5], producing output fields that demonstrate spatial coherence [6,9]. A narrow linewidth can be achieved by coupling the atoms slowly, though this obviously comes at the expense of beam flux [10]. In optical lasers, high spectral flux is generated through a competition between a depletable pumping mechanism and the damping. This causes a higher pumping rate to give a narrower output spectrum as well as higher total flux [11]. An atom laser with gain narrowing must also have a saturable pumping mechanism that operates at the same time as the damping [7]. Although it might be expected that an atom laser would behave most like an optical laser when the two-body interactions are minimum, we show that unless the pumping mechanism is sufficiently spatially selective, this interaction is actually necessary for a stable single-mode operation.

Multimode models of atom lasers using the Gross-Pitaevskii equation [12] are capable of including the spatial effects of the atomic field and the interatomic interactions [13], and are required to determine whether pumped lasers approach a single-mode operation. It was shown in [14] that the lasing mode of an atom laser with spatially independent pumping is unstable below a critical value of the interaction strength.

As for optical lasers, if the lasing system can be accurately described as a single mode, then the quantum statistics of that mode control the linewidth of the output beam. This means that, although a semiclassical model is useful to determine the stability of an atom laser, a full quantum-mechanical model must be used to calculate the linewidth of the beam coming from a pumped atom laser. Including the quantum statistics of the field dramatically increases the complexity of the model, so current quantum theories have been limited to a small number of modes [15]. Therefore, these models cannot describe effects such as the non-Markovian nature of the output coupling [16], except under the approximation that the lasing mode itself is a single mode [17]. It is also difficult to include the effects of the atomic interactions in these models except as a perturbation. Atom laser linewidths will be limited by these interactions due to Kerr-like dephasing of the lasing mode [18], as well as by thermal effects [19].

In this paper we add a spatially dependent pumping mechanism to the model of [14]. We find that the spatially dependent pumping mechanism acts as a mode-selective source of gain, which can favor the ground state. We find that this pumping mechanism can stabilize the atom laser in an otherwise unstable regime. As the atom laser linewidths are expected to be limited by the atom-atom interaction strength, a sufficiently spatially dependent pumping mechanism may drastically improve the fundamental limit to the atom laser linewidth.

In the next section we introduce the general model used for our atom laser system. In Sec. III, we examine the stability criteria of the model in the absence of spatially dependent pumping, as first shown in Ref. [14]. In Sec. IV, we explain the physics behind the instability of the linear model, and in Sec. V we demonstrate how this instability can be avoided with spatially dependent pumping.

II. ATOM LASER MODEL

In this section we introduce a multimode model for an atom laser and discuss its strengths and weaknesses. We have extended the model of [14] to include a mode-selective pumping mechanism. We model the atom laser in one dimension as a two-component semiclassical atomic field coupled to an incoherent reservoir of atoms described by a density $n(\mathbf{x})$. The first field, $\psi_t(\mathbf{x})$, is trapped in a harmonic potential and will form the lasing mode. The second field, $\psi_u(\mathbf{x})$, is untrapped and will form the laser beam. The pumping

*Electronic address: Simon.Haine@anu.edu.au

mechanism becomes mode-selective by introducing a coupling coefficient, $\kappa(\mathbf{x})$, between the incoherent reservoir and the lasing mode with a spatially dependent profile. The fields obey an equation of the Gross-Pitaevskii form, with damping due to one- and two-body loss, and reservoir coupling acting as a source of gain. The dynamical equations for the coupled system are

$$i\frac{d\psi_t}{dt}=\left[-\frac{\hbar}{2M}\nabla^2+\frac{V_t}{\hbar}-i\gamma_t^{(1)}+\left(\frac{U_{tt}}{\hbar}-i\gamma_t^{(2)}\right)|\psi_t|^2+\left(\frac{U_{tu}}{\hbar}-i\gamma_{tu}^{(2)}\right)|\psi_u|^2+\frac{i}{2}\kappa(x)n(x)\right]\psi_t+\kappa_R e^{i\mathbf{k}\cdot\mathbf{x}}\psi_u,$$

$$i\frac{d\psi_u}{dt}=\left[-\frac{\hbar}{2M}\nabla^2+\frac{Mgx}{\hbar}+\left(\frac{U_{uu}}{\hbar}-i\gamma_u^{(2)}\right)|\psi_u|^2+\left(\frac{U_{tu}}{\hbar}-i\gamma_{tu}^{(2)}\right)|\psi_t|^2\right]\psi_u+\kappa_R e^{-i\mathbf{k}\cdot\mathbf{x}}\psi_t,$$

$$\frac{dn}{dt}=r-\gamma_p n(x)-\kappa(x)|\psi_t|^2 n(x)+\lambda\nabla^2 n(x), \qquad (1)$$

with

$$\kappa(x)=\kappa_0 e^{-x^2/\sigma^2}, \qquad (2)$$

where M is the mass of the atom, V_t is the trapping potential, and g is the acceleration due to gravity, which is assumed to be along the x direction. $U_{ij}=4\pi\hbar^2 a_{ij}/M$ is the interatomic interaction between ψ_i and ψ_j, a_{ij} is the scattering length between those same fields, $\gamma_i^{(1)}$ is the loss rate of ψ_i due to background gas collisions, $\gamma_i^{(2)}$ is the loss rate of ψ_i due to two-body inelastic collisions between particles in that state, $\gamma_{tu}^{(2)}$ is the loss rate of each field due to two-body inelastic collisions between particles in the other electronic state, κ_R is the coupling rate between the trapped field and the output beam, $\mathbf{k}$ is the momentum kick due to the coupling process, κ_0 is the coupling coefficient between the incoherent atomic cloud $n(x)$ and the trapped field, σ is the parameter that controls the width of the coupling envelope, r is the rate of density increase of the incoherent cloud, γ_p is the loss rate from the incoherent cloud, and λ is the spatial diffusion coefficient. Periodic boundary conditions were enforced on the pumping reservoir to avoid diffusive loss of reservoir atoms.

The pumping terms in the above equations are phenomenological, describing an irreversible pumping mechanism from a reservoir which is assumed to be at a constant temperature. The reservoir can be depleted, but is replenished at a steady rate. These two features are necessary for any pumping mechanism that generates gain-narrowing through the competition of the gain and loss processes of the lasing mode. λ is chosen such that the diffusion is sufficient to make $n(x)$ approximately flat, with any irregularities being quickly filled in. In the low diffusion limit, the multimode behavior of the model is quite different, as the pumping favors gain into the excited states.

We have not included three-body losses, which are normally important. However, near a Feshbach resonance they may be negligible, as for ^{85}Rb, and still allow a wide range for the scattering length [20]. Both two-body and three-body loss act as a form of nonlinear damping. It is this nonlinear damping which is the origin of the instability presented in this paper, and the results of this paper are not affected by our choice to operate in the regime where the two-body loss is dominant.

It has been shown that output coupling can induce a localized bound state [17]. When the atom laser is pumped, the population of this bound state increases indefinitely. Gravity must be included in the model to make this state decay and allow steady-state operation to be achieved. For a given set of parameters, there is a maximum coupling rate κ_R below which this metastable state has a negligible effect on the total dynamics.

III. SPATIALLY INDEPENDENT PUMPING

We found in [14] that the atom laser model with spatially independent pumping ($\sigma=\infty$) was unstable in the absence of repulsive nonlinear interactions. With repulsive interactions included, we found that there was a critical interaction strength, above which the system was stable, with all excited modes damped. Increasing the pumping rate above this threshold caused faster damping of the excited modes.

We found that the semiclassical intensity fluctuations of the atom laser beam followed the dynamics of the lasing mode. For the range of output coupling rates that we consider, we found in our previous work that the condensate dynamics is very weakly affected by the output coupled beam [14]. Hence, in order to reduce the computational load, it is possible to ignore the output coupling. We do this for the following calculations. This means that we only gain information about the stability of the lasing mode, and not the semiclassical energy spectrum resulting from the outcoupling process. One consequence of neglecting the effect of the output beam is that in its absence there are no symmetry-breaking terms, so only the even modes of oscillation are present in the simulation. In this approximation, our equations of motion for the system become

$$i\frac{d\psi_t}{dt}=\left[-\frac{\hbar}{2M}\nabla^2+\frac{V_t}{\hbar}+\left(\frac{U_{tt}}{\hbar}-i\gamma_t^{(2)}\right)|\psi_t|^2-i\gamma_t^{(1)}+\frac{i}{2}\kappa(x)n(x)\right]\psi_t,$$

$$\frac{dn}{dt}=r-\gamma_p n(x)-\kappa(x)|\psi_t|^2 n(x)+\lambda\nabla^2 n(x). \qquad (3)$$

We integrated Eqs. (3) numerically using a pseudospectral method with a Fourth-order Runge-Kutta time step [23] using the XMDS numerical package [24], and used the atomic properties and loss rates for ^{85}Rb near a Feshbach resonance, where the interatomic interaction can be tuned with magnetic fields. We use the following experimentally reasonable parameters for all subsequent calculations: $\gamma_t^{(1)}=7.0$

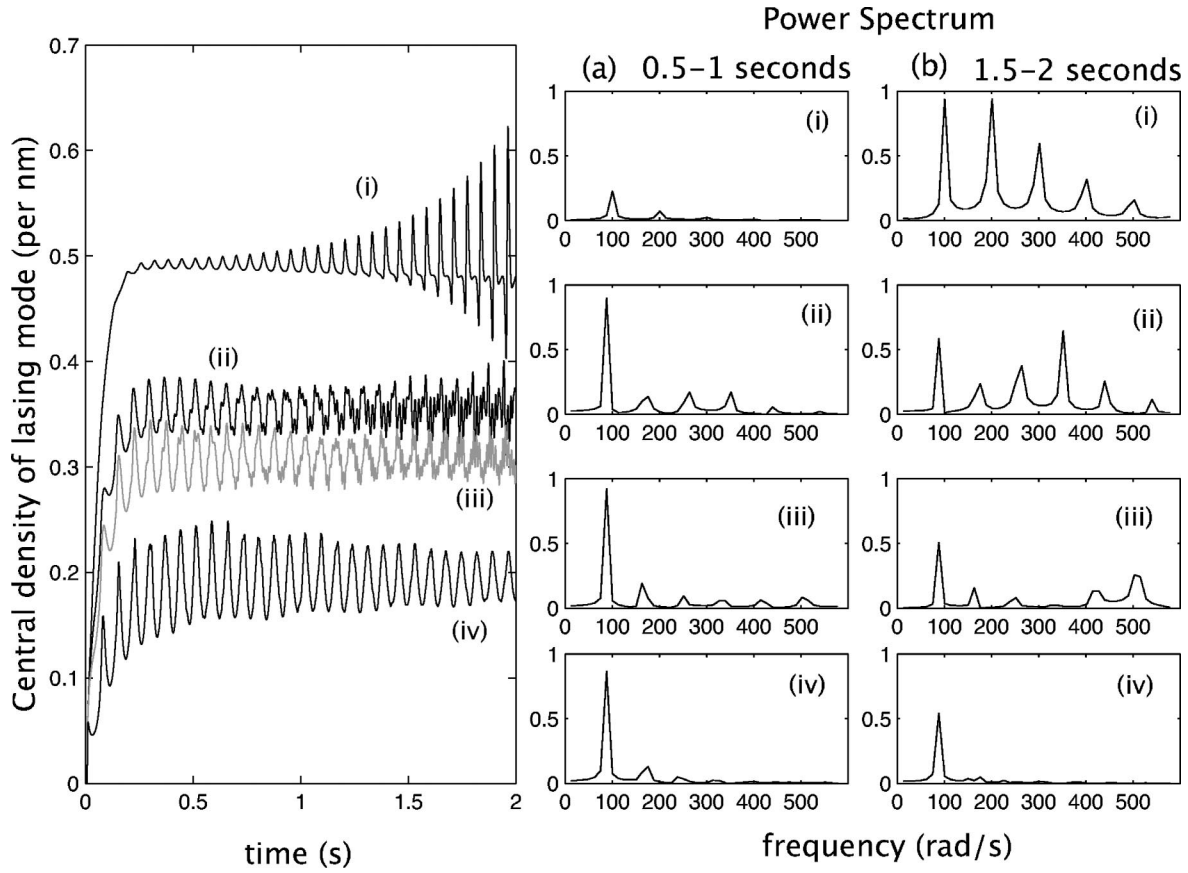

FIG. 1. Time series and power spectra of the laser mode central density. The pumping rate is $R=10^5\ \mathrm{s}^{-1}$. The scattering length is (i) $a_{tt}=0.01$ nm, (ii) $a_{tt}=0.5$ nm, (iii) $a_{tt}=1$ nm, and (iv) $a_{tt}=10$ nm. The spectral power is obtained from the time series from (a) $t=0.5-1.0$ s and (b) $t=1.5-2.0$ s.

$\times 10^{-3}\ \mathrm{s}^{-1}$, $\gamma_t^{(2)}=1.7\times 10^{-8}\ \mathrm{ms}^{-1}$, $\gamma_p=5\ \mathrm{s}^{-1}$, $\kappa_p=6.3\times 10^{-4}\ \mathrm{ms}^{-1}$, a trapping potential of $V_t=M\omega^2x^2/2$, where $\omega=50\ \mathrm{rad\,s}^{-1}$, and $\lambda=0.01\ \mathrm{ms}^{-1}$. The total pumping rate is $R=rL$, where L is the width of the pumping region.

Figure 1 shows the different regimes of stability as the scattering length is changed with a fixed pumping rate. The case with the lowest scattering length is unstable, with the breathing mode of oscillation growing without bound. The spectrum shows that all modes of oscillation are growing in amplitude. The systems with intermediate scattering length show a different type of behavior, with the lowest mode of oscillation (breathing) being damped, but higher modes increasing over time. The system with the highest scattering length is stable, with all excited modes being damped. The power spectrum shows a smooth transition from the even harmonic oscillator eigenfrequencies ($\Omega=n\omega$, n even) for the lowest scattering length, to the even Thomas-Fermi eigenfrequencies [13,21] [$\Omega=\omega\sqrt{n(n+1)/2}$, n even] for the highest scattering length. This suggests that for small values of the scattering length, the collective excitation of the condensate is approximated by eigenstates of the linear harmonic oscillator, while for large scattering lengths where the interatomic interaction dominates the energy, a linearized analysis such as found in [21] accurately describe the frequencies of the system. The collective excitation found by the method of [22] accurately describe the regime in between these two extremes.

We found it convenient to classify the behavior into three catagories. Type I behavior is where all excited modes are damped. In type II behavior, the breathing mode is damped but higher modes are undamped, so oscillations are initially decreasing, but the system is unstable over a long period. In type III behavior, all modes are undamped, and the system is unstable. We reproduce here the types of behavior found for different values of R and a (Fig. 2). For high pumping rates, the high-frequency oscillations produce numerical instabilities, so the boundaries in the phase diagram were difficult to explore in detail.

This behavior is a surprising departure from the analogy between optical lasers and atom lasers, as an optical laser is stable with zero interaction strength between the photons. In the following section, we analyze the system in the case of zero interaction strength and show why it is unstable.

IV. ANALYSIS OF STABILITY WITHOUT REPULSIVE INTERACTIONS

With the two-body repulsive interactions turned off there is no nonlinear phase diffusion so the quantum linewidth of the atom laser is expected to be a minimum, but we saw in the previous section that the semiclassical behavior of the atom laser was unstable. In this section we present a simplified analytical model which shows why the atom laser with no repulsive interactions is unstable, and demonstrate that a

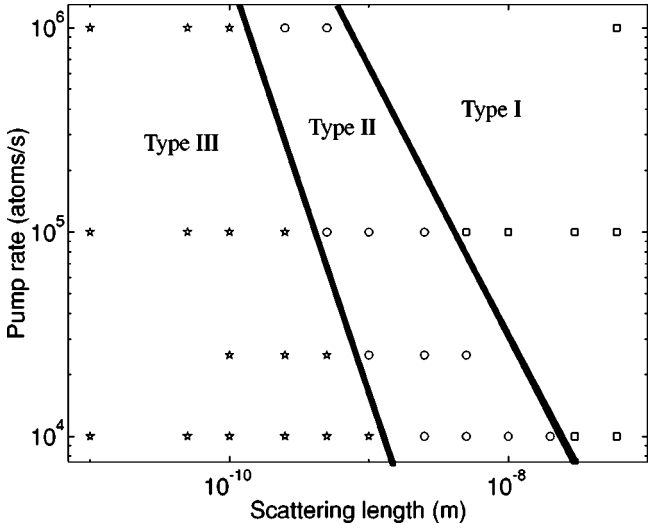

FIG. 2. This shows the regions of parameter space in which the atom laser is stable when the pumping is spatially independent ($\sigma=\infty$). The stable region (type I) is shown as squares, type II systems are shown as circles, and unstable (type III) systems are shown as stars.

spatially dependent pumping mechanism can stabilize the system, making an atom laser with minimum quantum noise a possibility. Our simplified model makes the assumption that there is infinite diffusion of the pump reservoir such that it has no spatial structure, and that the interaction between the output field and the lasing mode has a negligible effect on the behavior of the lasing mode. By setting $a_{tt}=0$ and ignoring the output beam, our equations for the system become

$$i\frac{d\psi_t}{dt}=\left(-\frac{\hbar}{2M}\nabla^2+\frac{V_t}{\hbar}-i\gamma_t^{(1)}-i\gamma_t^{(2)}|\psi_t|^2+\frac{i}{2L}\kappa(x)N_p\right)\psi_t, \tag{4}$$

$$\frac{dN_p}{dt}=R-\gamma_p N_p-\frac{N_p}{L}\int_{-\infty}^{\infty}\kappa_p|\psi_t|^2dx, \tag{5}$$

where we have assumed $n(x)$ takes the form

$$n=\frac{N_p}{L}\quad \text{for}\quad -L/2<x<L/2,$$
$$n=0\quad \text{otherwise}. \tag{6}$$

Expanding into the basis of harmonic oscillator eigenfunctions $\psi_t(x,t)=\Sigma_{n=0}^{\infty}c_n(t)\phi_n(x)$, where

$$\left\{\phi_n(x):\left(-\frac{\hbar^2}{2M}\nabla^2+V_t\right)\phi_n=E_n\phi_n\right\}$$

and solving for the mode coefficients, c_n, gives the equivalent set of equations,

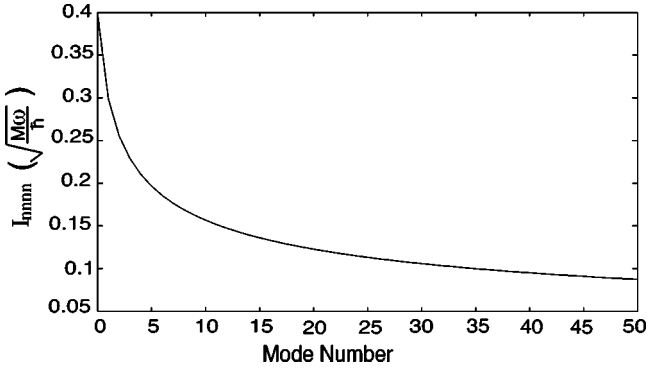

FIG. 3. Relative loss from each mode. I_{nnnn} (in units of $\sqrt{M\omega/\hbar}$) plotted against mode number n. The loss from each mode decreases for higher modes, so they will grow to a higher steady-state population.

$$\dot{c}_n=-\frac{i}{\hbar}E_n c_n+\frac{N_p}{2L}\sum_{m=0}^{\infty}\kappa_{mn}c_m-\gamma_t^{(1)}c_n-\gamma_t^{(2)}\sum_{ijk}c_i^*c_jc_kI_{nijk} \tag{7}$$

with $I_{nijk}=\int_{-\infty}^{\infty}\phi_n^*\phi_i^*\phi_j\phi_k dx$, $\kappa_{ij}=\int_{-\infty}^{\infty}\phi_i^*\kappa_p(x)\phi_j dx$, and $E_n=(n+\frac{1}{2})\hbar\omega$. In the $\sigma=\infty$ case, the system of equations is easier to analyze as they are diagonal in the gain term, i.e., $\kappa_{ij}=\kappa_p\delta_{ij}$. Making the transformation $b_n=c_ne^{i(E_n/\hbar)t}$ with $|b_n|^2=|c_n|^2$ equal to the number of atoms in mode n, and noting that the off-diagonal elements of I_{nijk} are small compared to the diagonal elements, gives

$$\dot{b}_n\approx\left(\frac{\kappa_p}{2L}N_p-\gamma_t^{(1)}\right)b_n-\gamma_{tt}^{(2)}I_{nnnn}|b_n|^2b_n. \tag{8}$$

The solution to Eq. (8) will grow until it is clamped by the two-body loss term. The steady-state population will be when

$$|b_n|^2=\frac{\frac{\kappa_p}{2L}N_p-\gamma_t^{(1)}}{\gamma_{tt}^{(2)}I_{nnnn}}.$$

Figure 3 shows the value of I_{nnnn} versus mode number n.

The loss rate decreases because the excited states are more spread out than the lower-energy states. This same trend occurs for three-body loss. The pumping is saturable and not mode-selective so the excited states have a higher net gain. The coupling between modes seeds the excited states, which become more populated than lower states. This growth is the origin of the atom laser instability.

A spatially dependent pumping mechanism would give unequal gain into each mode. The system would then be stable if the net gain (gain minus loss) into the ground state were higher than for all excited states.

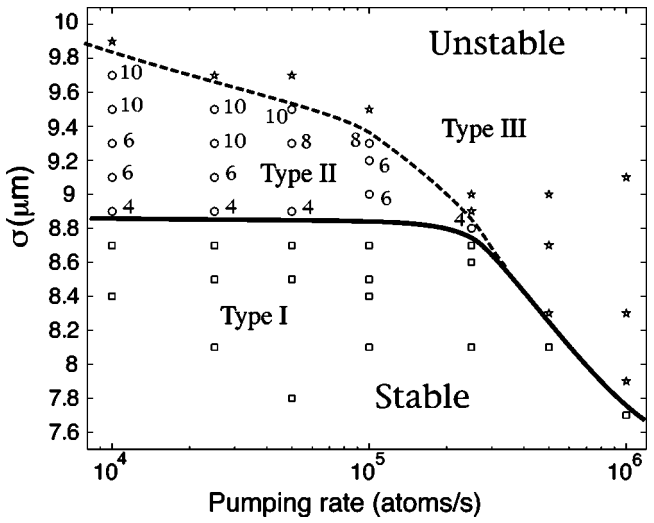

FIG. 4. Atom laser stability as a function of pumping rate and spatial extent of the pumping for zero interatomic interactions ($a=0$). Cases that displayed type I behavior are indicated with squares, cases that displayed type II behavior are indicated with circles, and type III behavior is indicated by stars. The region below the solid line is stable, the region above is unstable.

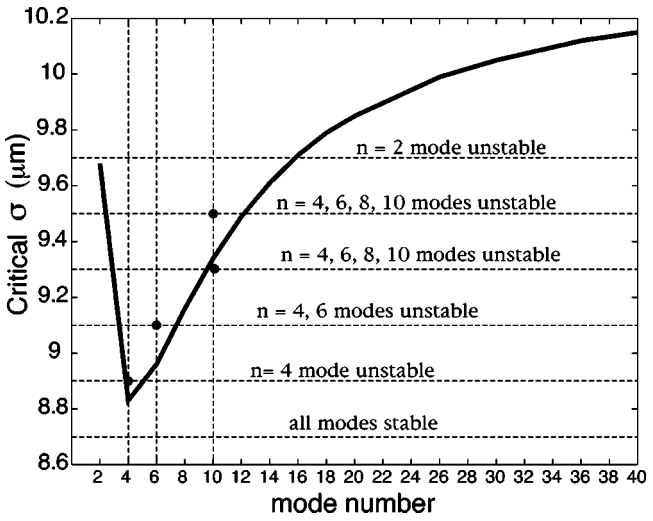

FIG. 5. Critical σ vs mode number. The bold line is obtained from setting $\langle d|c_n|^2/dt\rangle=0$ for $R=2.5\times10^4$ s^{-1}. This line represents the critical σ for each mode, above which the mode of oscillation is undamped, below which it is damped. The horizontal lines correspond to the $R=2.5\times10^4$ points from Fig. 4. The observed unstable frequencies agree with the multimode model. Type II behavior corresponds to the region between the minimum of the bold line and the critical σ for the $n=2$ mode of oscillation.

V. SPATIALLY DEPENDENT PUMPING

In the case of finite σ, there is unequal gain into each mode, so it may be possible to make the net gain into the ground state higher than for all excited states. Because the equations are more complicated due to the off-diagonal gain terms, our simple model of the previous section is inadequate to determine stability of the system. To test the stability, we integrate Eqs. (3) numerically using the same parameters as before, but with a finite value of σ.

Figure 4 shows the type of behavior found for different values of R and σ with $a_{tt}=0$. The system is found to be stable below a critical value of σ, with all excited modes being damped. This critical value decreases as the pumping rate is increased. Again, we found it convenient to classify the behavior into three categories. Type I behavior is where all modes are damped, type II behavior is where the breathing mode is damped, yet higher modes are undamped. The numbers next to the points in Fig. 4 indicate the highest undamped mode. In type III behavior, the breathing mode is undamped. Type II and III behavior differs from type II and III behavior in the absence of spatially dependent pumping, as there are only a finite number of undamped modes. This leads to the possibility of controlling the instability with feedback.

We can predict when the system will become stable by using a simplified two-mode model to determine when each excited mode of the system is damped. The system is determined to be stable when the ground state is stable against a small perturbation in each excited state. We are assuming that the amplitude of each excited mode is small enough such that they only interact with the ground state, and not each other. We assume an initial condition with a large population in the ground state, with a small perturbation in one of the excited modes. i.e., $\psi_{tt}=b_0\phi_0+b_n\phi_n$, $b_0=\sqrt{N_{lm}}, b_n=0.01b_0$, where $N_{lm}=\sqrt{R/2\gamma^{(2)}I_{0000}}$ is the approximate steady-state population of a stable lasing mode in the ground state. The equation governing the growth or decay of this excited mode is then

$$\begin{aligned}\dot{c}_n=&\frac{N_p(ss)}{2L}(\kappa_{n0}c_0+\kappa_{nn}c_n)-\gamma_t^{(1)}c_n\\&-\gamma_{tt}^{(2)}[c_n^*c_nc_nI_{nnnn}\\&+(c_0^*c_nc_n+c_n^*c_0c_n+c_n^*c_nc_0)I_{nnn0}\\&+(c_0^*c_0c_n+c_n^*c_0c_0+c_0^*c_nc_0)I_{nn00}\\&+(c_0^*c_0c_0)I_{n000}],\end{aligned}\tag{9}$$

where

$$N_p(ss)=\frac{R}{\gamma_p+\dfrac{\kappa_{00}N_{lm}}{L}}$$

is the approximate steady-state pump reservoir population. We test whether the system is stable against perturbation by checking the sign of $d|c_n|^2/dt=\dot{c}_n^*c_n+c_n^*\dot{c}_n$ time averaged over one cycle. Cases where $\langle d|c_n|^2/dt\rangle$ was determined to be negative are stable, as the system is returning to the steady state. Figure 5 shows the critical value of σ for each mode, above which the system is unstable. For the system to be stable, the system must be stable against perturbation from all excited modes, so σ must be below the critical σ for each mode.

The results obtained from the two-mode model agree with the behavior of the full model, with type I behavior corre-

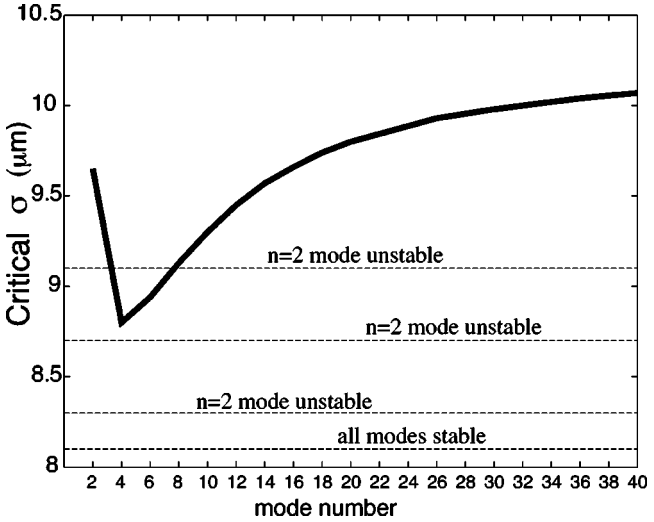

FIG. 6. Critical σ vs mode number for $R=5\times10^5\ \mathrm{s}^{-1}$. The four horizontal lines correspond to the four $R=5\times10^5$ points from Fig. 4. The bold line obtained from the two-mode model does not agree with the results obtained from the multimode model.

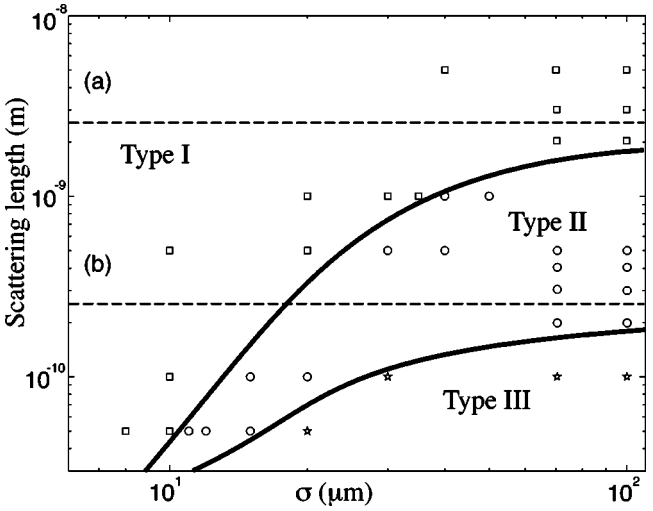

FIG. 7. Atom laser stability in σ and scattering length parameter space for $R=10^5\ \mathrm{s}^{-1}$. The stable region (type I) is shown as squares, type II systems are shown as circles, and unstable (type III) systems are shown as stars. The dashed lines represent the boundaries on the $\sigma=\infty$ plot for (a) type I and type II behavior, and (b) type II and type III behavior.

sponding to the region below the minimum of the bold line, type II behavior corresponding to the region between the minimum and the critical σ for the $n=2$ mode of oscillation, and type III behavior corresponding to the region above the critical σ for the $n=2$ mode of oscillation. This perturbative analysis ignores all but a single pair of modes in the system, and therefore would be expected to break down in the presence of significant nonlinearity. There is therefore a quite surprising level of agreement between this model and the full model, as seen in Fig. 5.

If we increase the pumping, however, the two-mode approximation breaks down. Figure 6 shows the critical σ obtained from the two-mode approximation for $R=5\times10^5\ \mathrm{s}^{-1}$. We believe that the discrepancy is between the full multimode model and the two-mode approximation is due to the larger population in the lasing mode causing the nonlinear loss term to act as a form of coupling between modes, causing the harmonic oscillator eigenmodes to become an inappropriate basis.

Finally, we investigate the effect of spatially dependent pumping on the atom laser model with repulsive nonlinear interactions present. We find that the nonlinear interactions drastically increase the width of the critical σ. This is because for high nonlinearity, the undamped modes have very small gain due to the spatially dependent pumping mechanism. Higher-order modes become damped without the spatially dependent pumping mechanism as the nonlinearity is increased, so the pumping envelope can become wider without allowing significant gain into the undamped modes. If it is difficult to produce a spatially dependent pumping mechanism experimentally, by including interactions it will be possible to obtain a stable atom laser with only a weak spatial dependence in the pumping mechanism.

Figure 7 shows the types of behavior found for finite values of a_{tt}, for $R=10^5\ \mathrm{s}^{-1}$. The system in the presence of repulsive nonlinear interactions does not require as much spatial dependence in the pumping mechanism to remain stable in the presence of nonlinear interactions. The boundaries between different regions of stability asymptote to the boundaries on the $\sigma=\infty$ phase plot, which are represented by the dashed lines.

VI. CONCLUSION

We have shown that a continuously pumped atom laser with no nonlinear repulsive interactions is unstable, but can be stabilized by a spatially dependent pumping mechanism. This is because the spatial dependence in the pumping mechanism causes a preference for pumping into the ground mode, to combat the effect of the nonlinear loss favoring the excited modes. There is a critical width to the pumping envelope, below which the system is stable, which depends on pumping rate and nonlinear interaction strength.

Current cooling techniques do not provide significant spatial selectivity on the length scale of the condensate. Indeed, no continuous pumping mechanism has been demonstrated. Therefore there may be significant experimental difficulty in providing an extremely spatially selective pumping mechanism, and some repulsive atomic interactions or feedback may be required to achieve modal stability.

ACKNOWLEDGMENTS

The Australian Centre for Quantum-Atom Optics is an Australian Research Committee Centre of Excellence. This work is also supported by the Australian Partnership for Advanced Computing (APAC) National Facility.

[1] M.R. Andrews, C.G. Townsend, H.-J. Miesner, D.S. Kurn, and W. Ketterle, Science **275**, 637 (1997).
[2] M.O. Mewes *et al.*, Phys. Rev. Lett. **78**, 582 (1997).
[3] J.L. Martin *et al.*, J. Phys. B **32**, 3065 (1999).
[4] I. Bloch, T.W. Hansch, and T. Esslinger, Phys. Rev. Lett. **82**, 3008 (1999).
[5] E.W. Hagley, L. Deng, M. Kozuma, J. Wen, K. Helmerson, S.L. Rolston, and W.D. Phillips, Science **283**, 1706 (1999).
[6] B.P. Anderson and M.A. Kasevich, Science **282**, 1686 (1998).
[7] H.M. Wiseman, Phys. Rev. A **56**, 2068 (1997).
[8] A. E. Siegman, *Lasers* (Oxford University Press, Mill Valley, CA, 1986).
[9] I. Bloch *et al.*, Nature (London) **403**, 166 (2000).
[10] J.J. Hope, Phys. Rev. A **55**, R2531 (1997).
[11] L. Mandel and E. Wolf, *Optical Coherence and Quantum Optics* (Cambridge University Press, Cambridge, 1995).
[12] F. Dalfovo *et al.*, Rev. Mod. Phys. **71**, 463 (1999); A.J. Leggett, *ibid.* **73**, 307 (2001).
[13] N.P. Robins *et al.*, Phys. Rev. A **64**, 043605 (2001).
[14] S.A. Haine *et al.*, Phys. Rev. Lett. **88**, 170403 (2002).
[15] H.M. Wiseman and M.J. Collett, Phys. Lett. A **202**, 246 (1995); H. Wiseman *et al.*, Quantum Semiclassic. Opt. **8**, 737 (1996); M. Holland *et al.*, Phys. Rev. A **54**, R1757 (1996).
[16] G.M. Moy *et al.*, Phys. Rev. A **59**, 667 (1999).
[17] J.J. Hope *et al.*, Phys. Rev. A **61**, 023603 (2000).
[18] H.M. Wiseman and L.K. Thomsen, Phys. Rev. Lett. **86**, 1143 (2001).
[19] R. Graham, Phys. Rev. Lett. **81**, 5262 (1998).
[20] J.L. Roberts, N.R. Claussen, S.L. Cornish, and C.E. Wieman, Phys. Rev. Lett. **85**, 728 (2000).
[21] B. Kneer, T. Wong, K. Vogel, W.P. Shleich, and D.F. Walls, Phys. Rev. A **58**, 4841 (1998).
[22] P.A. Ruprecht, M. Edwards, K. Burnett, and C.W. Clark, Phys. Rev. A **54**, 4178 (1996).
[23] The method, known as RK4IP, has been developed by the BEC theory group of R. Ballagh at the University of Otago. It is described in the Ph.D. thesis of B. M. Caradoc-Davies, which is online at http://www.physics.otago.ac.nz/bec2/bmcd/
[24] G. Collecutt, P.D. Drummond, and J.J. Hope, ''Extensible Multi-Dimensional Simulator,'' documentation and source available from http://www.xmds.org